tvst

Retina

Fundus Tessellation and Parapapillary Atrophy, as Ocular Characteristics of Spontaneously High Myopia in Macaques: The Non-Human Primates Eye Study

Jiaxin Tian[1,*], Jian Wu[1,2,*], Wei Liu[3], Kezhe Chen[2], Sirui Zhu[1], Caixia Lin[1], Hongyi Liu[1], Simeng Hou[1], Zhiwei Huang[4], Yingting Zhu[2], Ningli Wang[1], and Yehong Zhuo[2]

[1] Beijing Institute of Ophthalmology, Beijing Tongren Eye Center, Beijing Tongren Hospital, Capital Medical University, Beijing Key Laboratory of Ophthalmology and Visual Sciences, Beijing, China
[2] State Key Laboratory of Ophthalmology, Zhongshan Ophthalmic Center, Sun Yat-Sen University, Guangdong Provincial Key Laboratory of Ophthalmology and Visual Science, Guangzhou, China
[3] School of Food Sciences and Engineering, South China University of Technology, Guangzhou, China
[4] Guangzhou Huazhen Biosciences, Guangzhou, China

Correspondence: Ningli Wang, Beijing Institute of Ophthalmology, Beijing Tongren Eye Center, Beijing Tongren Hospital, Capital Medical University; Beijing Key Laboratory of Ophthalmology and Visual Sciences. No. 1 Dong Jiao Min Xiang Street, Dongcheng District, Beijing 100730, China. e-mail: wningli@vip.163.com
Yehong Zhuo, State Key Laboratory of Ophthalmology, Zhongshan Ophthalmic Center, Guangdong Provincial Key Laboratory of Ophthalmology and Visual Science, Sun Yat-Sen University, Guangzhou 510060, China. e-mail: zhuoyh@mail.sysu.edu.cn

Received: October 2, 2023
Accepted: January 24, 2024
Published: May 13, 2024

Keywords: nonhuman primates (NHPs); spontaneously high myopia, ocular characteristics, fundus tessellation, parapapillary atrophy (PPA)

Citation: Tian J, Wu J, Liu W, Chen K, Zhu S, Lin C, Liu H, Hou S, Huang Z, Zhu Y, Wang N, Zhuo Y. Fundus tessellation and parapapillary atrophy, as ocular characteristics of spontaneously high myopia in macaques: The non-human primates eye study. Transl Vis Sci Technol. 2024;13(5):8, https://doi.org/10.1167/tvst.13.5.8

Purpose: This study aimed to evaluate the ocular characteristics associated with spontaneously high myopia in adult nonhuman primates (NHPs).

Methods: A total of 537 eyes of 277 macaques with an average age of 18.53 $\pm$ 3.01 years (range = 5–26 years), raised in a controlled environment, were included. We measured ocular parameters, including spherical equivalent (SE), axial length (AXL), and intraocular pressure. The 45-degree fundus images centered on the macula and the disc assessed the fundus tessellation and parapapillary atrophy (PPA). Additionally, optical coherence tomography (OCT) was used to measure the thickness of the retinal nerve fiber layer (RNFL).

Results: The mean SE was -1.58 ± 3.71 diopters (D). The mean AXL was 18.76 $\pm$ 0.86 mm. The prevalence rate of high myopia was 17.7%. As myopia aggravated, the AXL increased ($r = -0.498$, $P < 0.001$). Compared with non-high myopia, highly myopic eyes had a greater AXL ($P < 0.001$), less RNFL thickness ($P = 0.004$), a higher incidence of PPA ($P < 0.001$), and elevated grades of fundus tessellation ($P < 0.001$). The binary logistic regression was performed, which showed PPA (odds ratio [OR] = 4.924, 95% confidence interval [CI] = 2.375–10.207, $P < 0.001$) and higher grades of fundus tessellation (OR = 1.865, 95% CI = 1.474–2.361, $P < 0.001$) were independent risk characteristics for high myopia.

Conclusions: In NHPs, a higher grade of fundus tessellation and PPA were significant biomarkers of high myopia.

Translational Relevance: The study demonstrates adult NHPs raised in conditioned rooms have a similar prevalence and highly consistent fundus changes with human beings, which strengthens the foundation for utilizing macaques as an animal model in high myopic studies.

Introduction

The global prevalence of myopia and high myopia is increasing yearly.[1] Within certain regions, myopic maculopathy has emerged as the most dominant cause of blindness, which leads to substantial economic losses and severe health detriments.[2–4] For a long time, animal models have been instrumental in elucidating pathogenesis, including species such as chickens,[5] mice,[6] guinea pigs,[7] tree shrews,[8] rabbits,[9] zebrafish,[10] macaques,[11] and marmosets.[12] Nonhuman primates (NHPs) exhibit close DNA homology and maintain highly conserved protein sequences with humans.[13] Their fundus structure, with the macula, is most similar to humans. Accordingly, they have a significant advantage in myopic maculopathy research.

In myopic research, form deprivation and lens-induced were standard methods for building myopia or axial elongation.[14,15] However, the natural occurrence of myopia is both limited and essential. Recent studies have demonstrated that macaques exhibit spontaneous ocular diseases resembling human age-related macular degeneration, high myopia, and glaucoma.[16,17] Tessellated fundus and choroidal neovascularization have been found in macaques' eyes with high myopia.[16] Ma et al. demonstrated that tessellated fundus and parapapillary atrophy (PPA) were the characteristic signs of myopia and had relationships with refractive errors in male macaques.[18] In clinical practice, myopia and high myopia have different clinical significance. Fundus tessellation and PPA were widely used in myopic population investigation and are regarded as pivotal features for high myopia. Do these markers retain their significance in NHPs' eyes with high myopia? What attributes are associated with them? A considerable number of macaques in the Non-Human Primates Eye Study (NHPES) study exhibited spontaneous high myopia.[19] Therefore, our study aimed to evaluate the ocular characteristics of macaques naturally experiencing high myopia. The findings may provide valuable insights for applying the animal model in highly myopic studies.

Methods

Animals

The NHPES was performed from 2021 to 2022 and aimed to delineate the ocular characteristics in NHPs.[19] All the macaques were from Huazhen Biosciences (HZ-Bio) company and held in Guangdong Province. The macaques were raised in air-conditioned rooms. The rooms were controlled within the temperatures from 16°C to 26°C and the relative humidity from 40% to 70%. The circadian rhythm is 12 hours. Drinking water, fresh fruits, and additional supplements were free to access. This study abided by the National Institutes of Health Guide for the Care and the Association for Research of Vision and Ophthalmology. The study was approved by the Ethical Committee of the Guangzhou Huazhen Biosciences Company (Ethics Number: 2020-168) and Zhongshan Ophthalmic Center (Permit Number: SYXK (YUE) 2018-0189). Based on the study, 305 adult macaques were randomly selected to evaluate the ocular feature of high myopia.

Systematic and Ophthalmic Examinations

Systematic and ophthalmic examinations were performed with the NHPs under anesthesia and based on a standardized protocol. Systematic characteristics, such as age, gender, and body weight, were recorded for analysis. Experienced ophthalmologists performed all ocular examinations. The structures of the ocular anterior segment were assessed by the slit-lamp biomicroscopy (TOPCON Slit-lamp SL-D701). The intraocular pressure (IOP) was measured 1 hour after anesthesia with an Icare tonometer (TA01i; Icare, Helsinki, Finland). Six measurements in three series were obtained to calculate the mean value. If the difference between each measurement exceeded 3 mm Hg, the result would be excluded.

A digital fundus scope (APS-BER Fundus Camera and FFA model, AITOMU) was used to obtain bilateral retinal 45-degree images of the macula (centered on the fovea) and the optic nerve (centered on the disc). Spectral-domain optical coherence tomography (OCT; Heidelberg Engineering GmbH, Heidelberg, Germany) was utilized to determine the thickness of the retinal nerve fiber layer (RNFL). The measurement range was a circular scan. The experienced operators adjusted the aiming circle to match the optic nerve head. The 24 radial scans were performed, covering a 3.6 mm diameter circle from 1.3 mm to 4.9 mm that included the parapapillary structure. The RNFL thickness was the average value of 360 degrees measures and was automatically calculated by the OCT software. Refractive status was measured under cycloplegia. One drop of 1% tropicamide was applied twice every 5 minutes for cycloplegia. Thirty minutes later, if the pupillary light reflex was still present or the pupil size was less than 6 mm, a third drop would be administered. Spherical equivalent (SE) was the mean value of three measurements and was calculated through

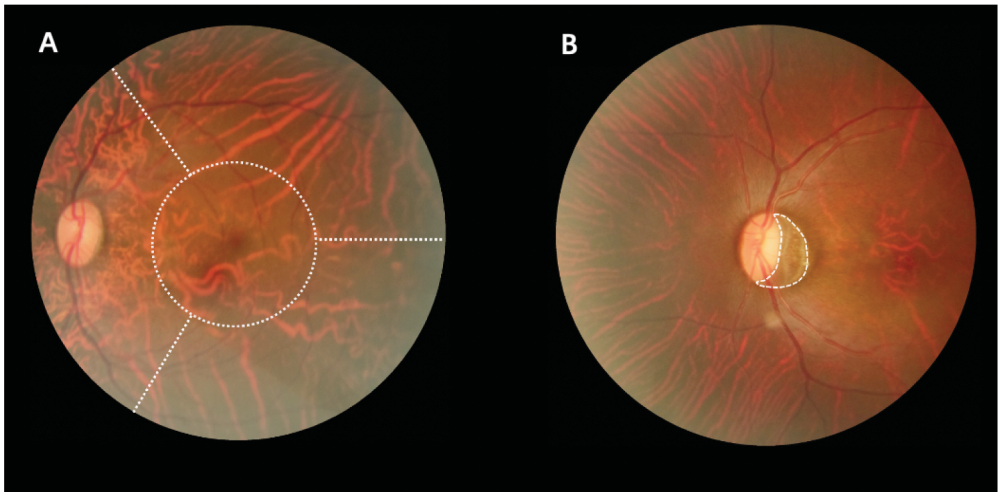

Figure 1. Fundus images analysis for tessellation and parapapillary atrophy (PPA). (**A**) The 45-degree fundus images centered on the macula were used to assess the condition of tessellation. The fundus was divided into four regions, including the macular, superior, inferior, and nasal. (**B**) The 45-degree fundus images centered on the disc were used to evaluate the PPA. The PPA was defined as the parapapillary zone with visible sclera and large choroidal vessels.

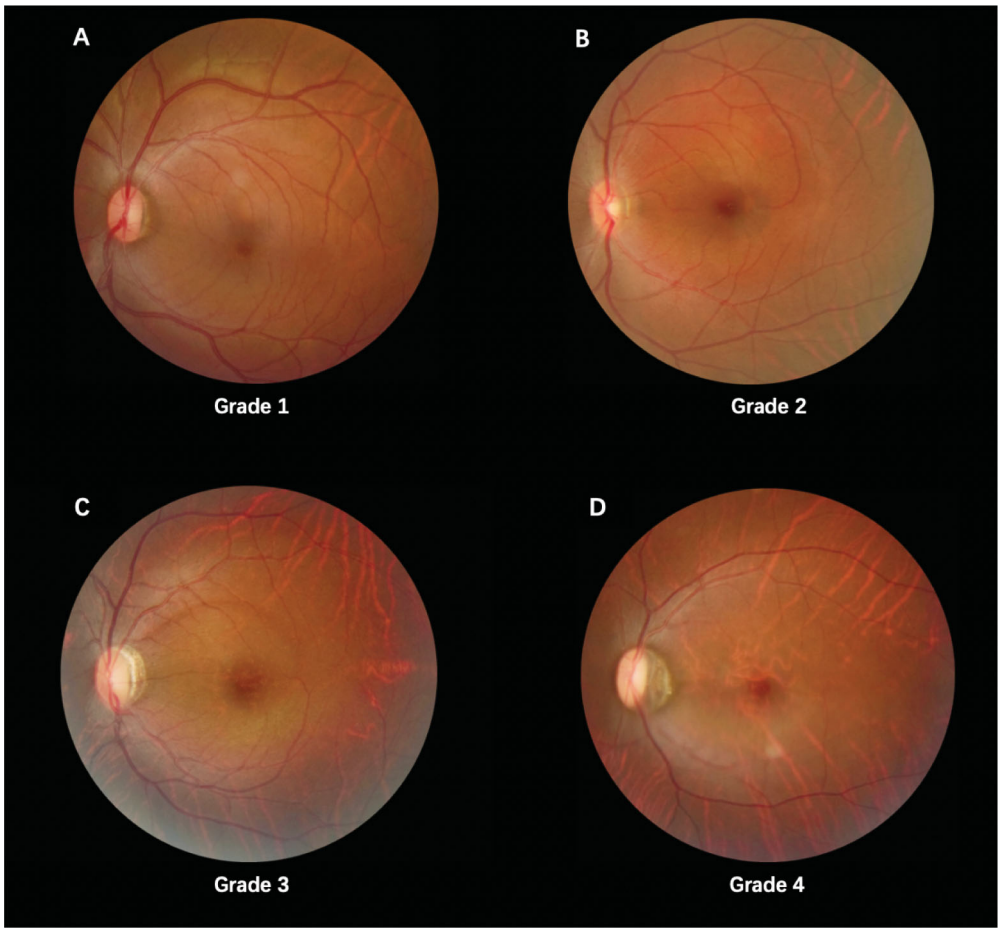

Figure 2. The evaluation of the grade of tessellation. Any region presenting more than three choroidal large vessels was defined as one grade for fundus tessellation. The final grade of tessellation was the accumulation of all the regions. (**A**) Grade 1 with the tessellation in the superior region. (**B**) Grade 2 with the tessellation in the superior and inferior regions. (**C**) Grade 3 with the tessellation in the superior, inferior, and nasal regions. (**D**) Grade 4 with the tessellation in the superior, inferior, nasal, and macular regions.

conventional formulas.[20]

$$SE = S + C/2$$

We defined SE as −5.00 D or less for high myopia.

The A-scan ultrasonography (Tomey AL-4000; Tomey, Nagoya, Japan) was used to get the axial length (AXL).

The detailed examination procedures have been described in the NHPES.[19]

Images Analysis

The 45-degree fundus images centered on the macula were used to assess the condition of tessellation. The fundus was divided into four regions (Fig. 1A), including the macular, superior, inferior, and nasal. Any region presenting more than three choroidal large vessels was defined as one grade for fundus tessellation. The final grade of tessellation was the accumulation of all the regions (Fig. 2). The 45-degree fundus images centered on the disc were used to evaluate the PPA. The PPA was defined as the parapapillary zone with visible sclera and large choroidal vessels (Fig. 1B). Two ophthalmologists (authors J.T. and J.W.) analyzed all the images independently. For results with disagreement, the more experienced retinal specialist (author C.L.) was consulted to make a final decision.

Statistical Analyses

Continuous variables were described using mean values (standard deviation) or median (interquartile range). Categorical data were presented as counts and frequencies. Spearman's rank correlation was performed to assess the relationship between two variables when at least one was a rank variable. An independent sample *t*-test with homogeneity of variances and a Mann Whitney *U* test were used to analyze significant differences between the eyes with and without high myopia for continuous variables with normal and abnormal distributions, respectively. One-way analysis of variance (ANOVA) was used to compare factors for three or more independent groups. Differences in categorical data were evaluated with the χ^2 test. The above comparisons between groups were regarded as univariate analyses for factors associated with high myopia or other characteristics. Multivariate logistic regression was then performed by including factors with *P* values ≤ 0.10 from univariate analysis to select the final independent variables with odds ratios (ORs) and 95% confidence intervals (CIs). All *P* values < 0.05 with 2-sided were considered statistically significant. Commercial software (SPSS version 24.0; SPSS, Inc., Chicago, IL, USA) was used for all statistical analyses.

Results

We initially selected 305 macaques, constituting a total of 610 eyes, for analysis in the study. After preliminary screening, 34 eyes were excluded due to the presence of fundus diseases, such as outer retinal atrophy, choroidal atrophy, retinal vascular occlusion, glaucoma, and anterior ischemic optic neuropathy. Nineteen eyes were eliminated for failure to measure refractive status or AXL due to pterygium, corneal diseases, or other media opacity. Twenty eyes were ruled out for being unable to assess fundus tessellation or PPA due to cataracts, corneal opacity, or images out of focus. Ultimately, the systemic and ocular parameters of 277 subjects, encompassing 537 eyes, were enrolled to analyze fundus characteristics of high myopia. Among them, 127 eyes belonged to male individuals. The average age was 18.53 ± 3.01 years (range = 5 to 26 years, median = 19 years, interquartile range = 18 to 20 years). The mean SE was −1.58 ± 3.71 diopters (D; range = −23.21 to 3.67 D, median = −0.33 D, interquartile range = −2.42 to 0.63 D), and the mean AXL was 18.76 ± 0.86 mm (range = 18 mm to 22.29 mm, median = 18.47 mm, interquartile range = 18.11 to 19.02 mm).

The systemic parameters of the subjects are presented in Table 1. The male subjects weighed more and had greater AXL compared to female subjects. However, there were no statistically significant differences in SE, fundus tessellation, and PPA between male and female subjects (see Tables 1, 2). Notably, the fundus tessellation and PPA conditions were nearly symmetrical in both eyes (see Table 2). SE demonstrated a negative correlation with the AXL, indicating that as SE decreased (myopia aggravation), AXL increased ($r = -0.498$, $P < 0.001$; Fig. 3).

Fundus tessellation was observed in 234 eyes (43.6%). Among these, superior tessellation exhibited the highest incidence (38.5%), followed by nasal tessellation (28.9%), inferior tessellation (27.2%), and then macular tessellation (17.1%). The grade of fundus tessellation was correlated with SE ($r = -0.464$, $P < 0.001$; Fig. 4A) and the AXL ($r = 0.466$, $P < 0.001$). Besides, the Kruskal-Wallis tests showed significant differences in age and RNFL thickness among eyes with different grades of tessellation ($P = 0.035$ and $P = 0.001$; see Supplementary Table S1, Fig. 4C). One hundred forty (26.1%) eyes showed PPA. Compared with eyes without PPA, eyes with PPA had less SE

Table 1. Systemic and Ocular Characteristics of the Macaques' Eyes

Variables	Male (Eyes = 127)	Female (Eyes = 410)	*P* Value
Age, y	19.00 (15.00 to 20.00)	19.00 (18.00 to 20.00)	0.540*
Body weight, kg	6.15 (5.34 to 6.92)	4.00 (3.62 to 4.60)	<0.001*
Intraocular pressure, mm Hg	20.00 (17.50 to 22.00)	19.00 (16.00 to 21.25)	0.035*
Spherical equivalent, D	−0.50 (−2.63 to 0.58)	−0.33 (−2.40 to 0.68)	0.312*
Axial length, mm	18.71 (18.33 to 19.49)	18.42 (18.10 to 18.97)	<0.001*
RNFL thickness, µm	92.50 (89.00 to 100.00)	93.00 (86.50 to 98.00)	0.131*

All data were shown as median (interquartile range).
RNFL, retinal nerve fiber layer.
*Mann–Whitney *U* test.
P is the result of the comparison between female and male NHPs.

Table 2. Fundus Tessellation and Parapapillary Atrophy of the Macaques' Eyes

	Male (Eyes = 127)			Female (Eyes = 410)				
	OD	OS	*P* Value	OD	OS	*P* Value	*P* Value[1]	*P* Value[2]
Parapapillary atrophy	17 (27.4%)	19 (19.2%)	0.821	49 (24.0%)	55 (26.7%)	0.533	0.587	0.690
Fundus tessellation								
Superior	28 (45.2%)	25 (38.5%)	0.444	76 (37.3%)	78 (37.9%)	0.899	0.264	0.931
Inferior	21 (33.9%)	18 (27.7%)	0.451	50 (24.5%)	57 (27.7%)	0.466	0.144	0.997
Nasal	26 (41.9%)	24 (36.9%)	0.563	51 (25%)	54 (26.2%)	0.778	0.010	0.096
Macular	13 (21.0%)	14 (21.5%)	0.937	32 (15.7%)	33 (16%)	0.926	0.331	0.306
The grade of fundus tessellation			0.663			0.812	0.177	0. 932
Grade = 0	30 (48.4%)	35 (53.8%)		119 (58.3%)	119 (57.8%)			
Grade = 1	5 (8.1%)	7 (10.8%)		27 (13.2%)	24 (11.7%)			
Grade = 2	7 (11.3%)	6 (9.2%)		16 (7.8%)	20 (9.7%)			
Grade = 3	11 (17.7%)	6 (9.2%)		18 (8.8%)	14 (6.8%)			
Grade = 4	9 (14.5%)	11 (16.9%)		24 (11.8%)	29 (14.1%)			

All data were shown as counts (frequencies).
P, Chi-square test for comparison between OD and OS; P^1, Chi-square test for comparison between female's OD and male's OD; P^2, Chi-square test for comparison between female's OS and male's OS.

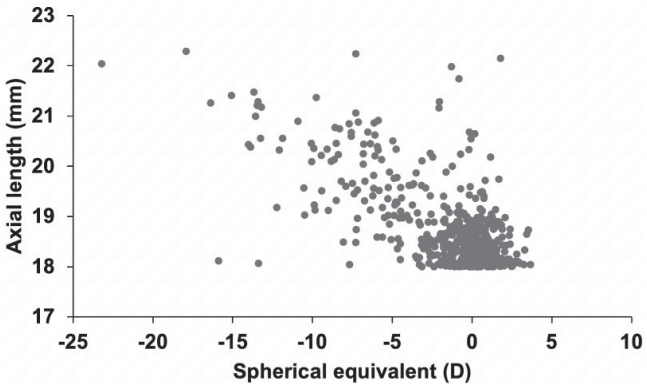

Figure 3. Scatterplots showed the correlation between spherical equivalent and axial length in the study.

($P < 0.001$; see Fig. 4B), longer AXL ($P < 0.001$), and thinner RNFL thickness ($P = 0.001$; Supplementary Table S2). No significant difference in age was observed between the eyes with and without PPA ($P = 0.320$; see Supplementary Table S2, Fig. 4D).

In the study, 82 eyes were identified as highly myopic. Compared with non-high myopia, highly myopic eyes had greater AXL ($P < 0.001$), less RNFL thickness ($P = 0.004$), a higher prevalence of PPA ($P < 0.001$), and higher grades of fundus tessellation ($P < 0.001$; Table 3). The tessellation rates in highly myopic eyes were higher than those in non-highly myopic eyes in all four regions (all $P < 0.001$; see Table 3). Binary logistic regression analyzed independent features for high myopia. Due to collinearity between SE and AXL and the close relationship between AXL and high myopia, AXL was ruled out. Beyond that, RNFL thickness, PPA, and grade of fundus tessellation were included as covariates. The result indicated that PPA (OR = 4.924, 95% CI = 2.375–10.207, $P < 0.001$) and higher grades of fundus tessellation (OR = 1.865, 95% CI = 1.474–2.361, $P < 0.001$; Table 4)

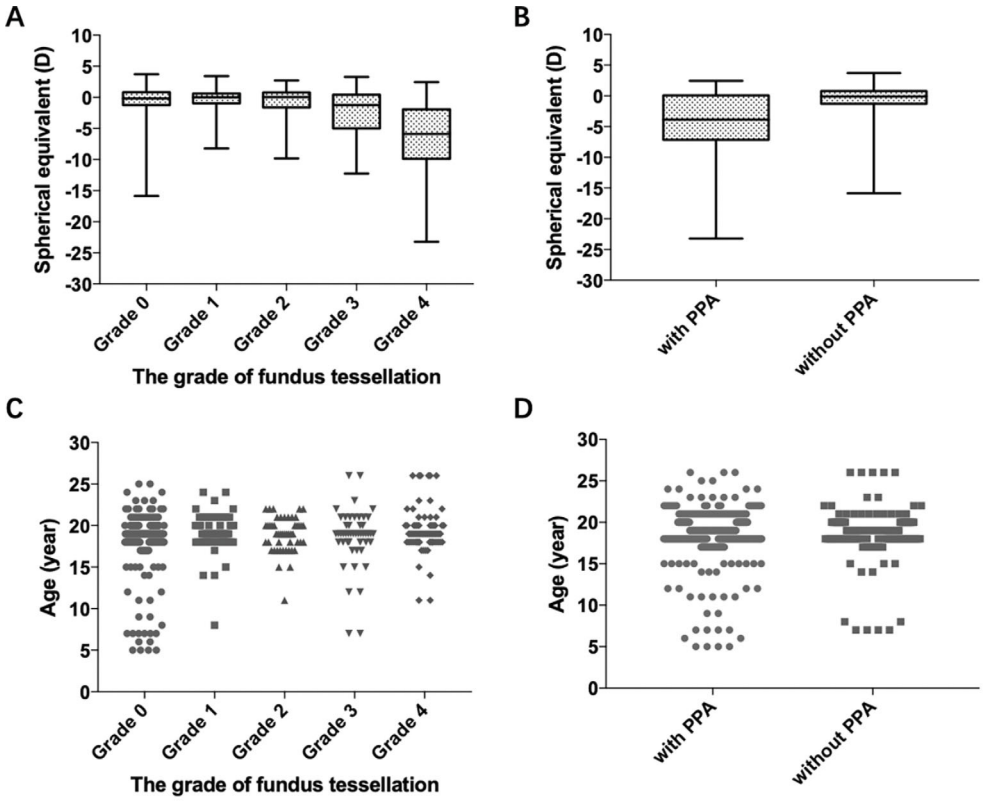

Figure 4. Distributions of spherical equivalent and ages in eyes with different fundus conditions. Spherical equivalent distribution among eyes with different grades of fundus tessellation (**A**) and in eyes with or without parapapillary atrophy (**B**). Age distribution among eyes with different grades of fundus tessellation (**C**) and in eyes with or without parapapillary atrophy (**D**).

were independent risk characteristics for high myopia. Additionally, ordinal logistic regression analysis and binary logistic regression analysis investigated independent factors for the grade of fundus tessellation and PPA, respectively. The results revealed that aging (OR = 1.102, 95% CI = 1.004–1.209, $P = 0.041$) and less SE (OR = 0.775, 95% CI = 0.722–0.833, $P < 0.001$; Supplementary Table S3) were significant factors for higher grades of fundus tessellation. Less SE was the independent risk factor for PPA (OR = 0.773, 95% CI = 0.705–0.848, $P < 0.001$; Supplementary Table S4).

Discussion

The study investigates the fundus characteristics of NHPs' eyes with naturally high myopia. Building upon previous findings demonstrating correlations between fundus tessellation, PPA, SE, and AXL, our investigation seeks to establish significant fundus tessellation and PPA as independent risk factors for high myopia in adult macaques. Aging was also associated with a higher grade of fundus tessellation. Additionally, it suggests a potential relationship between RNFL thickness and the development of PPA.

Among the 277 adult macaques screened, high myopia was observed in 49 subjects for a prevalence rate of 17.7%. The definition of high myopia in the population varies from study to study. The World Health Organization (WHO) and some research standardized to a SE of −5.00 D or less for high myopia.[1,21] Conversely, some literature adopts a definition of −6.00 D or less for high myopia.[22,23] Considering that macaques have more hyperopia than humans, we defined the boundary value of high myopia as −5.00 D. We believe it would be closer to the actual condition of high myopia in macaques. The incidence was similar to 20.2% among university students and 21% among 18-year-old individuals in regions with high myopia rates and higher than those in Israel, the United States, and some regions with relatively lower myopia rates.[24–27] All the macaques were raised in air-conditioned rooms with a 12 hour light/12 hour dark cycle. Lack of outdoor activities may be the primary reason for the significant incidence of high myopia. In the previous study, the rate of high myopia was 33%, higher than our result.[18] Different gender

Table 3. Systemic and Ocular Differences Between the Macaques' Eyes With and Without High Myopia

Variables	Non-High Myopia (Eyes = 455)	High Myopia (Eyes = 82)	*P* Value
Age, y	19 (18 to 20)	19 (17 to 21.25)	0.706*
Sex, male	106 (23.3%)	21 (25.6%)	0.650†
Body weight, kg	4.20 (3.70 to 5.20)	4.08 (3.60 to 4.76)	0.277*
Intraocular pressure, mm Hg	29.00 (17.00 to 21.25)	19.00 (16.00 to 23.00)	0.459*
Spherical equivalent, D	−0.04 (−1.08 to 0.79)	−7.69 (−10.19 to −6.20)	<0.001*
Axial length, mm	18.37 (18.08 to 18.75)	20.13 (19.29 to 20.67)	<0.001*
RNFL thickness, µm	93 (88 to 99)	90 (83 to 96.5)	0.004*
Parapapillary atrophy	84 (18.5%)	56 (68.3%)	<0.001†
Fundus tessellation			
Superior	147 (32.3%)	60 (73.2%)	<0.001†
Inferior	86 (18.9%)	60 (73.2%)	<0.001†
Nasal	100 (22.0%)	55 (67.1%)	<0.001†
Macular	43 (9.5%)	49 (59.8%)	<0.001†
The grade of fundus tessellation			<0.001†
Grade = 0	285 (62.6%)	18 (22.0%)	
Grade = 1	61 (13.4%)	2 (2.4%)	
Grade = 2	42 (9.2%)	7 (8.5%)	
Grade = 3	37 (8.1%)	12 (14.6%)	
Grade = 4	30 (6.6%)	43 (52.4%)	

All data were shown as median (interquartile range) or counts (frequencies).
RNFL, retinal nerve fiber layer.
*Mann–Whitney *U* test.
†Chi-square test.

Table 4. The Binary Logistic Regression Analysis for Ocular Characteristics Associated With High Myopia in the Macaques' Eyes

Variables	Odds Ratio (95% Confidence Interval)	*P* Value
Retinal nerve fiber layer thickness	0.996 (0.977 to 1.015)	0.663
Parapapillary atrophy	4.924 (2.375 to 10.207)	<0.001
The grade of fundus tessellation	1.865 (1.474 to 2.361)	<0.001

compositions between the two studies may contribute to the observed variations. In the previous study, all the macaques enrolled were male, whereas, in the current study, the proportion of females was higher than that of males (76.4% vs. 23.6%). Our findings revealed that male macaques had longer AXL than female macaques, which was likely attributed to their larger sizes and heavier body weights. This interpretation can also explain the significant difference in AXL rather than SE between male and female macaques. Besides, in the study by Ma et al., the age range was 13 years, from 8 to 21 years old, which was different from the current research. That might be the other reason for the discrepancy in the rate of high myopia. Ma et al. proposed that the AXL of rhesus macaques increases during their entire lifetime by surmising the AXL of rhesus macaques in previous investigations.[18] In our study, we did not observe a direct relationship between age and myopia in macaques from 5 to 26 years. Adult macaques might have finished the refractive development like human beings.[28] Alternatively, despite the age range spanning 21 years in the current study, half the subjects were between 18 and 20 years old. That would limit the sensitivity for detecting the relationship between age and diseases. The association between age and myopia might have been more pronounced if the age distribution of the subjects had been more distinct. In population studies, for every 1.00 D increase in myopia, the AXL is increased by 0.24 mm to 0.81 mm.[29–32] However, in our study, we did not observe severe axial elongation. Macaques have similar lens thickness and less corneal radius of curva-

ture than human beings. Corneal and lens factors might also participate in myopic development. Additionally, the absence of myopic eyes with noticeable pathologic changes, like myopic maculopathy or posterior staphyloma, might be the other reason for the rarity of axial elongation.

Fundus tessellation manifests as the increased visibility of the large choroidal vessel at the posterior fundus pole outside the peripapillary region.[33,34] The primary mechanism includes reduced choroid thickness and filling, increased intrachoroidal region pigmentation, and increased retinal pigment epithelium and choriocapillaris transparency.[33–36] In population studies, the grade of fundus tessellation serves as a proxy for choroidal thickness. It is also a significant characteristic of high myopia and represents the severity of myopic maculopathy.[37–39] In this study, we used the scope of tessellation to depict its feature and severity, establishing that a higher grade of fundus tessellation serves as a significant biomarker for high myopia in NHPs. In the preliminary observation of 45-degree fundus images centered on the macula, we observed that tessellations outside the macula were predominantly distributed in superior temporal, inferior temporal, and nasal. Therefore, we separated non-macular regions into three sections instead of standard quadrants similar to the Early Treatment Diabetic Retinopathy Study (ETDRS) grid to investigate the features of tessellations in NHPs. Regardless of the presence of high myopia, tessellation appeared more frequently in non-macular regions than macula regions. Besides, our assessment revealed that the severity of fundus tessellation increased with myopic aggravation and axial elongation. Population studies verified that fundus tessellation was also associated with primary open-angle glaucoma, age-related macular degeneration, and aging.[34,39,40] In the present study, we excluded the influence of glaucoma and other ocular diseases. Like humans, aging emerged as a crucial factor contributing to fundus tessellation in NHPs.

In population studies, PPA has been divided into four zones.[41] Alpha zones present Bruch's membrane and an irregularly structured retinal pigment epithelium with a high incidence in healthy populations.[41] Delta zones, characterized by elongated and thinned peripapillary scleral flanges, are prevalent in individuals with pathologic myopia. Recently, beta and gamma zones have garnered increased attention. Beta zones are described as the parapapillary zone with Bruch's membrane lacking retinal pigment epithelium (RPE), which is more associated with glaucoma. Gamma zones are defined as the parapapillary region without Bruch's membrane, which is more likely to have a relationship with axial elongation.[42] Both parapapillary zones are characterized as visible sclera and large choroidal vessels adjacent to the optic nerve head on fundus photographs and could only be distinguished by OCT.[41] This study assessed PPA through fundus images equivalent to the beta/gamma zone without specifying the particular PPA subtype related to high myopia. Our findings revealed that PPA was a significant feature of high myopia and might also be associated with RNFL thickness, a critical indicator for glaucoma. The results indirectly supported that PPA in NHPs has similar clinical significance to human beings.

Some previous studies have indicated the occurrence of myopia choroidal neovascularization and myopic foveoschisis in macaques.[16,43] In the preliminary screening, we also identified highly myopic eyes with retinal detachment or macular hemorrhage. However, the principal objective of the study was to investigate fundus characteristics for high myopia in adult macaques. Therefore, we excluded the subjects with other ocular diseases. The features of pathologic myopia, like posterior staphyloma and myopic maculopathy, could be verified in further studies.

Limitations of this study should be noted. As a cross-sectional study, we preliminarily demonstrated that fundus tessellation and PPA were significant indicators for highly myopic eyes of NHPs. A longitudinal study could provide more solid evidence for the relationship between the two characteristics and high myopia. Second, the structure of an optic disc and macula could be exhibited by OCT in detail, including choroidal thickness, retinal thickness, Bruch's membrane opening, and so on. The quantitative parameters related to fundus tessellation and PPA could be analyzed in future studies. Last, like human beings, beta and gamma zones in NHPs may have different clinical implications. The characteristics of different types of PPA, as well as the specific type of PPA associated with myopia, should be verified by OCT.

In conclusion, we reported the ocular characteristics of Chinese adult macaques with high myopia. The study demonstrated that the adult NHPs raised in air-conditioned rooms could develop spontaneously high myopia and had a similar prevalence to the population with a high prevalence of myopia. The SE was correlated with AXL. In NHPs, a higher grade of fundus tessellation and PPA were significant biomarkers of high myopia. The observed fundus changes in the eyes of NHPs with high myopia closely parallel those identified in human eyes, underscoring the translational relevance of macaques as an animal model for high myopic studies.

Acknowledgments

The authors thank Rongsheng Liao, Xiaorong Wu, Jingming Hu, Ziming Liao, Jiahe Song, Hanxiang Yu, and Liangzhi Xu for helping in the collection of monkey parameters. The authors also thank Xuehui Shi, MD, PhD, and Xiaoyan Peng, MD, PhD for giving advice for experiment design and diagnosis of ocular diseases.

Supported by grants from the National Key R&D Project of China (2020YFA0112701), the National Natural Science Foundation of China (82171057), the Science and Technology Program of Guangzhou, China (202206080005), the National Natural Science Foundation of China (GZR-2012–009), and the Major Science and Technology Project of Zhongshan City (2022A1007).

Disclosure: **J. Tian**, None; **J. Wu**, None; **W. Liu**, None; **K. Chen**, None; **S. Zhu**, None; **C. Lin**, None; **H. Liu**, None; **S. Hou**, None; **Z. Huang**, None; **Y. Zhu**, None; **N. Wang**, None; **Y. Zhuo**, None

* JT and JW contributed to this work equally and should be regarded as co-first authors.

References

1. Holden B, Fricke T, Wilson D, et al. Global prevalence of myopia and high myopia and temporal trends from 2000 through 2050. *Ophthalmology*. 2016;123(5):1036–1042.
2. Shen H, Zhang H, Gong W, et al. Prevalence, causes, and factors associated with visual impairment in a Chinese elderly population: the Rugao Longevity and Aging Study. *Clin Interv Aging*. 2021;16:985–996.
3. Fricke TR, Jong M, Naidoo KS, Sankaridurg P, Resnikoff S. Global prevalence of visual impairment associated with myopic macular degeneration and temporal trends from 2000 through 2050: systematic review, meta-analysis and modelling. *Br J Ophthalmol*. 2018;102(7):bjophthalmol-2017-311266.
4. Chang L, Pan CW, Ohno-Matsui K, et al. Myopia-related fundus Changes in Singapore adults with high myopia. *Am J Ophthalmol*. 2013;155(6):991–999.
5. Nickla DL, Wildsoet C, Wallman J. Visual influences on diurnal rhythms in ocular length and choroidal thickness in chick eyes. *Exp Eye Res*. 1998;66(2):163–181.
6. Tkatchenko TV, Shen Y, Tkatchenko AV. Mouse experimental myopia has features of primate myopia. *Invest Ophthalmol Vis Sci*. 2010;51(3):1297–1303.
7. Howlett MH, McFadden SA. Spectacle lens compensation in the pigmented guinea pig. *Vision Res*. 2009;49(2):219–227.
8. Metlapally S, McBrien NA. The effect of positive lens defocus on ocular growth and emmetropization in the tree shrew. *J Vis*. 2008;8(3):1.1–12.
9. Verolino M, Nastri G, Sellitti L, Costagliola C. Axial length increase in lid-sutured rabbits. *Surv Ophthalmol*. 1999;44(Suppl 1):S103–S108.
10. Shen W, Vijayan M, Sivak JG. Inducing form-deprivation myopia in fish. *Invest Ophthalmol Vis Sci*. 2005;46(5):1797–1803.
11. Hung LF, Crawford ML, Smith EL. Spectacle lenses alter eye growth and the refractive status of young monkeys. *Nat Med*. 1995;1(8):761–765.
12. Troilo D, Totonelly K, Harb E. Imposed anisometropia, accommodation, and regulation of refractive state. *Optom Vis Sci*. 2009;86(1):E31–E39.
13. Picaud S, Dalkara D, Marazova K, Goureau O, Roska B, Sahel JA. The primate model for understanding and restoring vision. *Proc Natl Acad Sci USA*. 2019;116(52):26280–26287.
14. Chakraborty R, Ostrin LA, Benavente-Perez A, Verkicharla PK. Optical mechanisms regulating emmetropisation and refractive errors: evidence from animal models. *Clin Exp Optom*. 2020;103(1):55–67.
15. Schaeffel F, Feldkaemper M. Animal models in myopia research. *Clin Exp Optom*. 2015;98(6):507–517.
16. Zeng B, Zhang H, Peng Y, et al. Spontaneous fundus lesions in elderly monkeys: an ideal model for age-related macular degeneration and high myopia clinical research. *Life Sci*. 2021;282:119811.
17. Pasquale LR, Gong L, Wiggs JL, et al. Development of primary open angle glaucoma-like features in a Rhesus macaque colony from Southern China. *Transl Vis Sci Technol*. 2021;10(9):20.
18. Ma Y, Lin Q, Zhao Q, Jin ZB. Prevalence and characteristics of myopia in adult Rhesus macaques in Southwest China. *Transl Vis Sci Technol*. 2023;12(3):21.
19. Wu J, Liu W, Zhu S, et al. Design, methodology, and preliminary results of the non-human primates eye study. *BMC Ophthalmol*. 2023;23(1):53.
20. Thibos L, Wheeler W, Horner D. Power vectors: an application of Fourier analysis to the description

and statistical analysis of refractive error. *Optom Vis Sci*. 1997;74(6):367–375.
21. Pan CW, Zheng YF, Anuar AR, et al. Prevalence of refractive errors in a multiethnic Asian population: the Singapore Epidemiology of Eye Disease Study. *Invest Ophthalmol Vis Sci*. 2013;54(4):2590–2598.
22. Ip JM, Huynh SC, Robaei D, et al. Ethnic differences in the impact of parental myopia: findings from a population-based study of 12-year-old Australian children. *Invest Ophthalmol Vis Sci*. 2007;48(6):2520–2528.
23. Pärssinen O, Kauppinen M. Risk factors for high myopia: a 22-year follow-up study from childhood to adulthood. *Acta Ophthalmol*. 2019;97(5):510–518.
24. Wei S, Sun Y, Li S, et al. Refractive errors in university students in Central China: the Anyang University Students Eye Study. *Invest Ophthalmol Vis Sci*. 2018;59(11):4691–4700.
25. Lin LL, Shih YF, Hsiao CK, Chen CJ. Prevalence of myopia in Taiwanese schoolchildren: 1983 to 2000. *Ann Acad Med Singap*. 2004;33(1):27–33.
26. Shneor E, Doron R, Ostrin LA, Gordon-Shaag A. The prevalence of refractive errors in college students in Israel. *J Optom*. 2022;15(4):284–292.
27. Pan CW, Klein BE, Cotch MF, et al. Racial variations in the prevalence of refractive errors in the United States: the multi-ethnic study of atherosclerosis. *Am J Ophthalmol*. 2013;155(6):1129–1138.e1121.
28. Rozema JJ, Ní Dhubhghaill S. Age-related axial length changes in adults: a review. *Ophthalmic Physiol Opt*. 2020;40(6):710–717.
29. Iyamu E, Iyamu J, Obiakor CI. The role of axial length-corneal radius of curvature ratio in refractive state categorization in a Nigerian population. *ISRN Ophthalmol*. 2011;2011:138941.
30. Hashemi H, Bouyeh A, Khabazkhoob M. Association between refractive errors and ocular biometry in an elderly population. *Optom Vis Sci*. 2023;100(1):74–81.
31. Olsen T, Arnarsson A, Sasaki H, Sasaki K, Jonasson F. On the ocular refractive components: the Reykjavik Eye Study. *Acta Ophthalmol Scand*. 2007;85(4):361–366.
32. Mallen EA, Gammoh Y, Al-Bdour M, Sayegh FN. Refractive error and ocular biometry in Jordanian adults. *Ophthalmic Physiol Opt*. 2005;25(4):302–309.
33. Jonas JB, Gründler A. Optic disc morphology in "age-related atrophic glaucoma". *Graefes Arch Clin Exp Ophthalmol*. 1996;234(12):744–749.
34. Chen H, Wen F, Li H, et al. The types and severity of high myopic maculopathy in Chinese patients. *Ophthalmic Physiol Opt*. 2012;32(1):60–67.
35. Yoshihara N, Yamashita T, Ohno-Matsui K, Sakamoto T. Objective analyses of tessellated fundi and significant correlation between degree of tessellation and choroidal thickness in healthy eyes. *PLoS One*. 2014;9(7):e103586.
36. Koh VT, Nah GK, Chang L, et al. Pathologic changes in highly myopic eyes of young males in Singapore. *Ann Acad Med Singap*. 2013;42(5):216–224.
37. Guo Y, Liu L, Zheng D, et al. Prevalence and associations of fundus tessellation among junior students from Greater Beijing. *Invest Ophthalmol Vis Sci*. 2019;60(12):4033–4040.
38. Cheng T, Deng J, Xu X, et al. Prevalence of fundus tessellation and its associated factors in Chinese children and adolescents with high myopia. *Acta Ophthalmol*. 2021;99(8):e1524–e1533.
39. Yan YN, Wang YX, Xu L, Xu J, Wei WB, Jonas JB. Fundus tessellation: prevalence and associated factors: the Beijing Eye Study 2011. *Ophthalmology*. 2015;122(9):1873–1880.
40. Spaide RF. Age-related choroidal atrophy. *Am J Ophthalmol*. 2009;147(5):801–810.
41. Wang YX, Panda-Jonas S, Jonas JB. Optic nerve head anatomy in myopia and glaucoma, including parapapillary zones alpha, beta, gamma and delta: histology and clinical features. *Prog Retin Eye Res*. 2021;83:100933.
42. Jonas JB, Fang Y, Weber P, Ohno-Matsui K. Parapapillary gamma and delta zones in high myopia. *Retina*. 2018;38(5):931–938.
43. Sin TN, Kim S, Li Y, et al. A spontaneous nonhuman primate model of myopic foveoschisis. *Invest Ophthalmol Vis Sci*. 2023;64(1):18.